HOKKAIDO UNIVERSITY

Title	Raman spectra measurements on DEPC liposome and cell membrane of living neuron under xenon pressure
Author(s)	Uchida, Tsutomu; Nagayama, Masafumi; Yamazaki, Kenji; Gohara, Kazutoshi; Sum, Amadeu K.
Citation	Canadian journal of chemistry, 93(8), 831-838 https://doi.org/10.1139/cjc-2014-0542
Issue Date	2015-08
Doc URL	http://hdl.handle.net/2115/59825
Type	article (author version)
File Information	Uchida150202CJC_revise.pdf

Instructions for use

Raman spectra measurements on DEPC liposome and cell membrane of living neuron under xenon pressure

Tsutomu Uchida[1*], Masafumi Nagayama[1,2], Kenji Yamazaki[1], Kazutoshi Gohara[1], Amadeu K. Sum[3]

1. Division of Applied Physics, Faculty of Engineering, Hokkaido University,

   N13 W8, Kita-ku, Sapporo 060-8628, Japan

2. Hokkaido University of Education Asahikawa Campus

3. Center for Hydrate Research, Department of Chemical & Biological Engineering, Colorado School

of Mines, 1600 Illinois St., Golden, CO, U.S.A.

* Corresponding author: E-mail: t-uchida@eng.hokudai.ac.jp, Tel&Fax: +81-11-706-6635

Abstract

Raman spectra of liposomes were measured under xenon pressures and low temperatures to observe the spectra changes accompanying the gel to liquid crystalline phase transition of the liposomes. C-H stretching bonds of the lipids in the liposome were slightly red shifted at approximately 285 K and atmospheric pressure, which coincided well with the phase transition condition. This Raman-peak shift was observed at lower temperatures and related linearly to the xenon pressures. The xenon pressure dependence on the phase transition temperature was in good agreement with the DSC measurements, and the red shifts of Raman peaks supported the molecular mechanism of interaction between xenon and phospholipid bilayers suggested by the MD simulations. The phase-transition measurements under xenon pressure with the microscopic Raman spectroscopy were applied to cultured neuronal networks to observe the interaction of dissolved xenon with the cell membrane and the surrounding water.

(143 words)

Key words

Liposome, Neuron, Raman shift, Phase transition, Xenon,

Introduction

Xenon (Xe) is the noble gas known to be a potent general anesthetic gas. General anesthesia is exhibited through the depression of nerve function, but the specific molecular mechanism by which anesthetic agents induce an anesthetic state remains poorly understood. One of the molecular mechanisms of general anesthesia which has been studied for over a century is known as the Mayer-Overton correlation. This model suggested that anesthetic gases dissolve in the lipid bilayer of neurons to reduce the ion-channel activity.[1,2] Later, another molecular mechanism of general anesthetic was proposed by Pauling[3] and Miller[4]. In their mechanism, they noted that anesthetic gases were the guest molecules of clathrate hydrates, and suggested a mechanism by which the gas would block the diffusion of signal-transmitting molecules at the synaptic junction by forming clathrate structures. In order to study the effect of Xe on the neuronal activities, Uchida et al.[5] measured the firing of neuronal networks under Xe-gas pressure. They observed that the synchronized bursts in the neuronal network were inhibited when exposed to Xe-gas pressure while the single firing of neuron survived. They considered that the guest gases of clathrate hydrates could induce a structuring of the liquid phase in the synaptic junction to inhibit the diffusion of signal-transmitting molecules even though clathrate hydrates were not formed. A third molecular mechanism was proposed as the direct interaction between anesthetic gases and hydrophobic pockets or clefts in proteins, especially integral membrane proteins such as gated-ion channels.[6] Based on the experimental investigations[7-15] and molecular simulations,[16] the target ion-channels have been selected. However, a consistent molecular mechanism has not been proposed yet. Therefore, more physico-chemical approaches besides biological experiments are required to understand the interaction between anesthetic gases and biomolecules.

Booker and Sum[18] investigated the interaction of Xe with model phospholipid membranes using molecular dynamics (MD) simulations of pure dioleoylphoshatidyl choline (DOPC) bilayers with Xe at a range of concentrations and pressures. The simulations revealed that Xe atoms exerted broad biophysical changes on the membrane fluidity, the lateral pressure profiles near the lipid head groups, and the bilayer structure by substantially increasing the lipid head groups spacing

and bilayer thickness. Booker and Sum[18] also measure the gel-liquid crystalline phase transition temperature (T_m) of a model membranes (dielaidoyl-phosphatidylcholine: DEPC) under Xe pressures by a high-pressure differential scanning calorimetry (HP-DSC). The HP-DSC measurements showed the pressure effect on T_m of DEPC liposomes was opposite compared to previous reports.[19] Thus they discussed the effect of Xe dissolved in the liquid bilayers on the phase-transition temperatures. Following their studies, Uchida and Sum[20] constructed an experimental system for Raman spectroscopic measurements on DEPC liposomes under Xe pressure to observe the change in the Raman shifts around T_m.

In the present study, we show the Xe pressure effect on T_m of DEPC liposomes, which suggested that the specific pressure effect on T_m is caused by Xe. This physico-chemical approach is useful to interpret the complex results of Raman spectra of actual neurons. Then we perform microscopic Raman spectra on cultured rat cortical neurons under Xe pressures. The results suggest that the cell membranes of neurons under Xe pressures exhibit effects similar to those observed in liposomes. Therefore, we confirm that Xe dissolves into the neuron cell membrane, which then modify the fluidity of the membrane during the pressurization.

Experimental Section

Sample preparation

The preparation procedure for the liposomes in solution was similar to that in previous studies.[18,20] Here we briefly present the procedure. As the model lipid, 18:1 (Δ9-Trans) phosphocholine (DEPC) in powder form (Avanti Polar Lipids, Inc., Alabama, U.S.A.) was used for the liposome (large multilamellar vesicles) solution by dissolving 20 mg/mL of powdered DEPC lipids into deionized and deuterated water (99.9%, Sigma–Aldrich, St. Louis, U.S.A.). Deuterated water was used for preparing liposome solutions to distinguish the Raman spectra of liposome from that of water. Lipids were mixed vigorously for one hour and the liposomes were then allowed to age overnight at room temperature, approximately 300 K, which was above the DEPC phase transition temperature, T_m = 285 K.[21]

The typical features of DEPC liposomes (large multilamellar vesicle) are shown in Fig. 1. The optical microscopic image (Fig. 1a) indicates that the vesicles (1~10 μm diameter) are formed in solution although they are partly aggregated. The FEG-TEM image of the vesicle (Fig. 1b) shows that the typical size of the vesicle ranged from sub-microns to several microns in diameter. This is consistent with the optical microscopic observations. The cross-section of a vesicle was observed by fracturing part of the surface as shown by the thick arrow in Fig. 1b. This figure shows that the vesicle is multilamellar (at least 10 layers), and each layer has a thickness of approximately 20 nm. Since each lipid bilayer is approximately 4 nm,[18] this thickness includes the water between the bilayers.

The preparation procedure for neuron samples were almost the same as that in our previous studies.[5,22] Dissected cortex was prepared from Wister rats at embryonic day 17 using the Nerve-Cell Culture System (Sumitomo Bakelite, Tokyo, Japan), as described previously.[23-25] Cortices were dissociated into single cells using dissociation solution (mainly papain), and then re-suspended in Neuron Culture Medium (Sumitomo Bakelite; serum-free conditioned medium from 48-h rat astrocyte confluent cultures based on Dulbecco's modified Eagle's minimum essential medium (DMEM)/F-12 with N2 supplement[24,25]). Dissociated neuron was plated with a nominal density of approximately 5000 cells/mm² onto a poly(ethylenimine)-coated glass dish (12 mm in outer diameter) fit for the high-pressure vessel.

The cultures were incubated in the neuron culture medium in a humidified atmosphere containing 5% carbon dioxide and 95% air at 310 K. After 3 days in the neuron culture medium (twice a week), half of the medium was replaced with fresh DMEM/serum medium, which consisted of DMEM (Invitrogen-Gibco, Carlsbad, U.S.A.) supplemented with 5% fetal bovine serum (Invitrogen-Gibco), 5% horse serum (Sigma–Aldrich), 25 μg/mL insulin (Invitrogen-Gibco), 100 U/mL penicillin, and 100 μg/mL streptomycin (Invitrogen-Gibco).[22] Thus, the Neuron Culture Medium is gradually replaced with the DMEM/serum medium during culture. The adhesion, growth, and morphological changes of cultured neurons were observed under a phase-contrast microscope (Olympus, Tokyo, Japan; type CKX-41). After approximately two weeks, the neurons constructed the robust network with frequent spontaneous firings.[5,22] So we used the cultured

neurons for Raman spectroscopic measurements after three-week culture (Fig. 2).

Experimental Procedure

Raman spectra were measured with a Renishaw inVia Reflex micro-Raman system (250 mm single monochrometer-type, at the Open Facility, Hokkaido University Sousei Hall) with 532 nm semi-conductor laser through the microscope equipped with the long-working distance objective lens (Olympus, Tokyo, Japan; type LMPlanFLN x50). The incident laser beam had a diameter of less than 5 μm, and its power was approximately 10 mW. The scattered radiation was collected through a slit with 180-degree geometry at 70 μm and dispersed by a 1800 mm^{-1} grating. The CCD detector (1024 x 256 channels) was used for the Raman signal detection. The Raman spectrum of the silicon wafer (520 cm^{-1}) was used for the correction of the wavenumber measurement and the estimation of the resolution of Raman shift as the full-width at half maximum of the silicon peak, which was approximately 2.3 cm^{-1}. Each Raman spectrum was obtained by three consecutive measurements with 10 s accumulation for DEPC liposomes and with 60 s accumulation for neurons. For the spatial averaging and to reduce the risk of sample damage with laser radiation, Raman spectra at more than three positions for each condition was collected and averaged. The spectrum of the neon-emission was used for the correction of the wavenumber measurement. Since the C-H stretching modes of Raman spectra for neurons overlapped by the tale of the O-H stretching mode, a peak deconvolution process was not appropriate. Thus, the peak deconvolution process was applied only for a limited number of spectra in the present study.

Approximately 100 μL of the DEPC liposome solution was introduced to the high-pressure vessel (Taiatsu Techno Co., Tokyo, Japan) equipped with sapphire glass windows. The neuronal samples cultured for more than three weeks were also used for the Raman spectroscopic measurements. In order to reduce the large background owing to the auto fluorescence of the medium, we replaced the solution with approximately 100 μL of Hank's Balanced Salt Solution (HBSS buffer, Invitrogen-Gibco) prior to the Raman measurements. We confirmed the survival of neurons in the HBSS buffer for the period of the Raman measurements. The sample temperature was controlled from 293 to 270 K by a refrigeration unit (Thermo Fisher Scientific, NH, U.S.A.; type

AC-150), which was monitored with a thermocouple (T-type, ±0.3 K). The high-pressure vessel was connected to gas cylinders (99.995% pure Xe, and 99.9% pure N_2) supplied by Hokkaido Air Water Inc. (Sapporo, Japan) and pressurized via a regulator up to 1 MPa with fluctuations less than ±0.02 MPa after flushing the air remaining in the cell for a few times initially. Temperature and pressure readings were recorded with a data logger (Graphtech Co., Yokohama, Japan; type GL220).

The sample temperature was decreased from room temperature or increased from the lowest temperature in each run in stages at approximately 2 K per 15~20 min. To observe the reverse phase transition with pressure, the gas was applied after reaching a temperature lower than T_m at atmospheric pressure. Conversely, the depressurization was done when the temperature increased above T_m at that pressure during the temperature ramping process. The typical temperature and pressure conditions during an experimental run are shown in Fig. 3.

Results and Discussion

Raman spectra of DEPC liposomes under Xe pressure

Typical Raman spectra of DEPC liposomes during the temperature decrease process in a specific run are shown in Fig. 4. Based on the peak assignment for DEPC,[20] we observed both Raman spectra of DEPC, such as C-N symmetric stretching mode (approximately 715 cm^{-1}), methylene C-C stretching mode (triple peaks between 1030 and 1150 cm^{-1}), CH_2 twist mode and bending mode (at around 1300 and 1440 cm^{-1}, respectively), and methylene C-H stretching mode (triple peaks between 2800 and 3100 cm^{-1}), and deuterated water (O-D stretching mode between 2100 and 2800 cm^{-1}) with some background peaks owing to the glass cells (lower than 500 cm^{-1} and around 900 cm^{-1}). These figures also show that each spectrum changed slightly with changing pressure and temperature conditions.

Since the previous studies suggested that the obvious Raman shift change on DEPC liposomes was observed in the methylene C-H stretching modes during the phase transition between liquid crystalline and gel states, we focused on the peak positions of triple peaks observed between 2800 and 3100 cm^{-1}: the C-H symmetric stretching mode (lowest wavenumber around 2850

cm^{-1}), the C-H anti-symmetric stretching mode (middle wavenumber around 2880 cm^{-1}) and the terminal CH$_3$ symmetric stretching mode (highest wavenumber around 2920 cm^{-1}).[20,26] Figure 5 shows the extended Raman spectra at the C-H stretching mode region during the temperature decrease process (temperature from 292.8 to 278.8 K, pressure from 0 to 0.5 MPa). These spectra show that the peak at 2850 cm^{-1} shifted to lower wave numbers by approximately 3 cm^{-1} in the lower temperature phase, and that the peak at 2890 cm^{-1} sharpened while shifting to lower wave numbers by approximately 5 cm^{-1}.

To determine the phase change temperatures, these peak positions were plotted as a function of temperature at atmospheric pressure and at 0.50 MPa Xe pressure, as shown in Fig. 6. This figure shows that both peak positions shifted to lower wave numbers at the same temperature. During the temperature decrease at atmospheric pressure, the phase transition occurred at approximately 285 K. When a Xe pressure of 0.50 MPa was applied at that temperature, the Raman spectra returned to that of the higher temperature phase. Then the phase transition occurred again at approximately 281 K with further temperature decrease at 0.50 MPa Xe pressure. Therefore, we determined these temperatures as the phase transition temperatures T_m under both pressures, and confirmed that the phase transition of DEPC liposomes under Xe pressure is reversible.

We also determined T_m at other pressure conditions. Figure 7 shows that T_m [K] decreases linearly with increase in Xe pressure, P_{Xe} [MPa], which can be mathematically described as (correlation factor $R^2 = 0.97$):

$$T_m = 285.2 - 7.67 \ P_{Xe} \tag{1}.$$

A linear extrapolation of $P_{Xe} = 0$ MPa results in a T_m coinciding well with the phase transition temperature of DEPC.[21] The previous data obtained by HP-DSC[18] is in good agreement with this temperature dependence, as shown by solid diamonds in Fig. 7. This figure also shows that T_m was slightly increased under 0.76 MPa N$_2$ pressure (solid triangle) compared to that under atmospheric pressure. This is the opposite tendency with Xe pressure, but coincided with the hydrostatic pressure dependence on T_m for liposomes.[19] It is also noticed that T_m was approximately 282 K under 0.89 MPa N$_2$-Xe mixed gas pressure (open circle). When we consider the partial pressure of Xe in the mixed gas, approximately 0.33 MPa, the shift of T_m agrees well with equation (1), as

shown by the arrow. Therefore, we conclude that T_m of DEPC liposome shifted to lower temperatures by application of Xe pressure into the system.

For the O-D stretching mode of DEPC liposome solutions (Fig. 8), no peak position changes on the two main peaks (approximately 2370 and 2500 cm^{-1}) were observed during the experimental runs. This result suggests that there was no solid phase present in the focused area even though the pressure and temperature conditions were stable for Xe hydrates. However, we found that the relative peak intensity of the Raman peak at 2370 cm^{-1} standardized by that at 2500 cm^{-1} increased slightly with decreasing temperature. This tendency was consistent with previous reports on pure water or lipid dispersions,[27,28] which can be associated with the development of a hydrogen-bonding network in liquid (water structuring). Since we could not find an obvious gap in the peak intensity ratio during the experimental run, such as observed in the C-H stretching mode of the Raman spectra, we concluded that the phase transition process of DEPC liposomes has insignificant effect on the surrounding water hydrogen-bonding network.

For the lower Raman shift region (lower than 2000 cm^{-1}, Fig. 4a), there are several Raman peaks derived from the DEPC molecules in the liposomes. The noticeable changes on the Raman spectra were only observed on the C-C stretching mode at the approximately 1065 and 1090 cm^{-1} peaks. These peaks were assigned as the methylene C-C stretching mode of the *trans* and *gauche* conformations in the lipid acyl chains, respectively, and the relative intensity ratio of these peaks are known to be a measure of the ordering of the lipid tails in the liposomes.[29] Unfortunately, most of peaks around 1000 cm^{-1} had low signal/noise ratio due to the background noise from the silica glass plate used at the bottom of the glass dish, and we could not analyze the changes in peak intensity quantitatively. However, we identified that these peaks shifted to slightly lower wave numbers during the experiments. These peak shifts, resulting from the phase transition,[29] support the results obtained from the C-H stretching mode described above.

In the present study, we observed the peak shifts to lower wave numbers on both the C-H symmetric stretching mode (~2850 cm^{-1}) and the C-H anti-symmetric stretching mode (~2890 cm^{-1}) of DEPC molecules in the phase transition of the liposomes from liquid crystalline to gel phase. The shift of T_m depended linearly on the partial pressure of Xe and not on N$_2$. Compared to these peaks,

9

the peak position of the terminal CH$_3$ symmetric stretching mode was unchanged. Thus, we suggest that the stretching vibrations of lipid tail of DEPC become slower in the gel phase compared to the liquid crystalline phase, and that the lateral vibrations of lipid tail are more sensitive than the longitudinal vibrations.

Molecular dynamics simulations suggested that Xe dissolved in the phospholipid bilayer preferentially localized in the hydrophobic core of the bilayer and increased the membrane fluidity owing to decreasing interactions between the lipid molecules.[24] They also described that dissolved Xe increased the local ordering of the lipid acyl chains in the region between the *cis* double bonds and the terminal carbons, straightened the tail, and induced an increase in the head group spacing. These molecular models are consistent with the Raman spectra change obtained in the present study. Therefore, it is adequate to conclude that Xe dissolved in solution under pressure preferentially localize in the tail area where the DEPC layers meet (bilayer core), which results in an increasing in the fluidity of the liposomes while inducing local ordering of the hydrophobic core.

Raman spectra of neurons under Xe pressure

The typical Raman spectra of cultured neurons during the temperature decrease process in a specific run are shown in Fig. 9. Since neurons stuck to the bottom of the glass cell in thin and stretched conditions, the signal intensity was relatively weak and the background peaks from the glass plate was relatively large (Fig. 9a). In addition, the C-H stretching modes of the neurons overlapped with the large band corresponding to the O-H stretching mode of water in the HBSS buffer (Fig. 9b). In order to investigate the Raman spectra change of neurons during the experimental run, we analyzed the Raman spectra by subtracting the background of the glass plates for the peaks lower than 1200 cm^{-1} and the O-H stretching modes for the peaks for the C-H stretching mode. By doing such procedure, we confirmed triple peaks in the region between 2800 and 3000 cm^{-1} (Fig. 10), which are assigned as the C-H symmetric stretching mode (approximately 2850 cm^{-1}), the C-H anti-symmetric stretching mode (approximately 2885 cm^{-1}), and the terminal CH$_3$ symmetric stretching mode (approximately 2935 cm^{-1}), based on the analogy of the Raman spectra for DEPC liposomes. We observed that, as in the DEPC liposome experiments, both 2850

cm^{-1} and 2885 cm^{-1} peaks shifted to slightly lower wave numbers (approximately 3 cm^{-1}) during the experiment, although the 2935 cm^{-1} peak remained relatively unchanged. Since in neurons the cell membrane is not composed by a simple phospholipid, like in the DEPC liposomes, it was considered that the cell membrane would not have a well-defined phase transition temperature. However, in the present experimental conditions, we observed a discontinuity in the peak position change with temperature as observed in the DEPC liposome. Based on the analogy to the liposome experiments, we consider this discontinuity point as the phase transition temperature of neuronal cell membranes (T_m). As such, we estimated T_m'at several Xe pressure conditions. Figure 11 shows that the estimated T_m'tends to decrease with increasing Xe pressure. This is consistent with the results for DEPC liposomes (shown as a dashed line in Fig. 11), although both the variation of T_m'and the uncertainty of each estimate are larger. Therefore, the results suggest that the fluidity of neuronal cell membrane increase with Xe dissolved in the membrane, depending on the Xe partial pressure.

We also examined the change of the Raman spectra of the O-H stretching mode for the samples with the neurons. As shown in Fig. 12, the peak positions of two noticeable peaks (approximately 3270 and 3400 cm^{-1}) are relatively unchanged during the experimental runs. This suggests that no other water phase formed during the experiments. However, it is also observed that their intensity ratio changed with temperature and pressure. When we examined the temperature dependence on the intensity ratio, it generally increased with decreasing temperature, as observed for the DEPC liposomes. At Xe pressures higher than 0.3 MPa, on the other hand, we recognized an anomalous increase in the intensity ratio at a specific temperature (T_w). Based on the analogy of Raman spectra for the C-H stretching mode, we considered that this sudden change in Raman intensity ratio of O-H stretching mode resulted from the phase transition of the neuron cell membrane. However, the pressure dependence of T_w indicates the opposite tendency to that of T_m' (Fig. 13), that is, T_w increases with increasing Xe pressure. We found that this pressure dependence on T_w coincided well with the equilibrium condition of Xe hydrate,[30] although there was no evidence for the existence of Xe hydrate crystals, as mentioned above. Thus, we concluded that the Raman spectra change in O-H stretching mode was related to the development of a hydrogen-bonding network of water around neurons, which was accelerated by the localization of Xe close to the cell

11

membrane.

For the Raman spectra at lower wave numbers, lower than 2000 cm^{-1} (Fig. 9a), we observed several peaks related to the neurons. Some of them were assigned in previous studies: around 750 cm^{-1} from cytochrome C,[31] around 1000 cm^{-1} from C-C aromatic ring of phenylalanine,[32,33] around 1440 cm^{-1} from C-H deformation vibration[34] or CH$_2$ deformation[35], and around 1660 cm^{-1} from Amide I.[32-34] We examined the temperature dependence of these visible peaks but most of them did not significantly changed throughout the experiments, or signal intensities were not large enough to examine the peak position change compared to noise. The C-C stretching mode of Raman spectra of neurons were very weak compared to those observed in DEPC liposomes, so they were poor indicators of the membrane structure for the neuronal network sample in the present experimental system.

Based on the Raman spectroscopic measurements on the cultured neuronal network, we found that the cell membrane would change its physical properties under Xe pressure and low temperature. This is caused by the dissolved Xe in the membrane, as observed in the DEPC liposomes. We should then consider the effect of dissolved Xe in the neuronal cell membrane in the context of general anesthesia. Since dissolved Xe in the membrane is consistent with the Meyer-Overton correlation, the ion-channel activity may be reduced. Uchida et al.[5] observed, however, that the simple firing activity of neurons were unchanged during Xe pressurization. Thus, it is possible that the dissolved Xe in the cell membrane can change the physical properties of lipid bilayers of neuron, but only have little effect on the electrical signal generation in the neuron.

In addition, we found that the hydrogen-bonding network around the neuronal network was affected under Xe pressure. Although we confirmed no crystalline phases in the experimental system, the anomalous development of the hydrogen-bonding network can be enhanced by the dissolved Xe. Since the solubility of Xe in the solution is limited, and no significant changes were observed in the DEPC liposomes, the observed water structuring was caused by Xe located near the neuronal cell membrane. Water molecules existing in nano-size domains (less than 100 nm) tend to structure and are often difficult to crystallize.[36] This tendency was also observed in gas hydrate systems.[36-38] Such kinds of nano-size domains existed in the neuronal network, such as the synaptic

12

junctions. As such, we considered that the Xe-induced development of the hydrogen-bonding network observed by Raman spectra in the neuronal network system may occur under supercooled conditions of Xe hydrates and preferentially at the boundary between the neurons. This is consistent with the molecular mechanism of general anesthesia (the modified clathrate model) proposed by Uchida et al.[5]

Therefore, it is concluded that Xe applied to the cultured neuronal network can dissolve not only into the neuronal cell membrane to modify its structural and dynamics properties, but also into the solution existing between neurons to develop an enhanced hydrogen-bonding network of water molecules. Both effects can contribute to the Xe-induced inhibition of synchronized bursts observed in a cultured neuronal network, and consequently to the molecular mechanism of general anesthesia.

Conclusions

Raman spectroscopic observations were performed on both DEPC liposome solutions and cultured neuronal networks under Xe pressures up to 0.8 MPa and temperatures below room temperature. As a model cell membrane, DEPC liposomes provided various information about the interaction between Xe and phospholipid molecules. Some of the Raman peaks for the C-H stretching mode and C-C stretching mode of DEPC molecules were found to shift towards lower wave numbers in the gel to liquid crystalline phase transition. The phase transition temperature of DEPC liposomes was found to linearly decrease with increasing Xe partial pressure. This pressure dependence on the phase transition temperature coincided well with a previous study with the high-pressure differential scanning calorimetry.[18] These results suggested that dissolved Xe preferentially accumulate in the hydrophobic area of the DEPC bilayer, causing an increase in the lipid bilayer fluidity and induce local ordering of the lipid tails.

Based on the molecular model suggested from the present Raman spectroscopic observations and previous MD simulations on the DEPC liposomes, we demonstrated Raman spectroscopic observations on cultured neuronal network under Xe pressures. Although the neuron

cell membrane was a complex mixture of phospholipid molecules, Raman spectra results suggested that Xe dissolved into the cell membrane can change their physical properties under certain conditions, a result similar to the gel-to-liquid crystalline phase transition of DEPC liposomes. Moreover, we found the Xe-induced development of hydrogen-bonding network around the neurons. This phenomenon was observed at Xe pressures higher than 0.3 MPa and lower than the dissociation temperature of Xe hydrate. Since there was no evidence of Xe hydrates formed in the system during the experiments, this water structuring might preferentially occur in the narrow space between neurons, such as the synaptic junctions.

These findings suggest that Xe applied to the cultured neuronal network preferentially dissolved into the cell membrane and localized in the narrow space between neurons, thus affecting not only changes in the physical properties of cell membrane but also development of an enhanced hydrogen-bonding network in the synaptic junction. The combination of studies involving these spectroscopic observations with electric measurements on the cultured neuronal network has the potential to provide unique evidence to gain further insight into the molecular model of general anesthesia.

Acknowledgements

References

(1) Mayer, H. *Naunyu-Schmiedeberg's Arch Pharmacol.* **1899**, 42, 109.

(2) Overton, C.: Studien uber die Narkose: Zugleich ein Beitrag zur Allgemeinen Pharmakologie (Verlag von Gustav Fischer, Jena), 1901.

(3) Pauling, L.: *Science* **1961**, 134, 15.

(4) Miller, S. L. *Proc. Natl. Acad. Sci.* **1961**, 47, 1515.

(5) Uchida, T.; Suzuki, S.; Hirano, Y.; Ito, D.; Nagayama, M.; Gohara, K. *Neuroscience* **2012**, 214, 149. doi: 10.1016/j.neuroscience.2012.03.063.

(6) Franks, N. P.; Lieb, W. R. *Nature* **1984**, 310, 599.

(7) Franks, N. P.; Dickinson, R.; de Sousa, S. L. M.; Hall, A. C.; Lieb, W. R. *Nature* **1998**, 396, 324.

(8) de Sousa, S. L. M.; Dickinson, R.; Lieb, W. R.; Franks, N. P. *Anesthesiology* **2000**, **92**, 1055.

(9) Ma, D.; Wilhelm, S.; Maze, M.; Franks, N. P. *British Journal of Anaesthesia* **2002**, 89, 739.

(10) Plested, A. J. R.; Wildman, S. S.; Lieb, W. R.; Franks, N. P. *Anesthesiology* **2004**, 100, 347.

(11) Nagele, P.; Metz, L. B.; Crowder, C. M. *Anesthesiology* **2005**, 103, 508.

(12) Dinse, A.; Fohr, K. J.; Georgieff, M.; Beyer, C.; Bulling, A.; Weigt, H. U. *British Journal of Anesthesia* **2005**, 94, 479.

(13) Preckel, B.; Weber, N. C.; Sanders, R. D.; Maze, M.; Schlack, W. *Anesthesiology* **2006**, 105, 187.

(14) Haseneder, R.; Kratzer, S.; Kochs, E.; Eckle, V-S.; Zieglgansberger, W.; Rammes, G. *Anesthesiology* **2008**, 109, 998.

(15) Georgiev, S. K.; Furue, H.; Baba, H.; Kohno, T. *Molecular Pain* **2010**, 6, 25.

(16) Dickinson, R.; Peterson, B. K.; Banks, P.; Simills, C.; Martin, J. C. S.; Valenzuela, C. A.; Maze, M.; Franks, N. P. *Anesthesiology* **2007**, 107, 756.

(17) Uchida, T.; Oshita, S.; Ohmori, M.; Tsuno, T.; Soejima, K.; Shinozaki, S.; Take, Y.; Mitsuda, K. *Nanoscale Research letters* **2011**, 6, 295. doi: 10.1186/1556-276X-6-295.

(18) Booker, R. D.; Sum, A. K. *Biochim. Biophys. Acta* **2013**, 1828, 1347. doi: 10.1016/j.bbamem.2013.01.016.

(19) Srinivasan, K. R.; Kay, R. L.; Nagle, J. F. *Biochemistry,* **1974**, 13, 3494.

(20) Uchida, T.; Sum, A. K. *Low Temp. Sci.* **2013**, 71, 105. http://hdl.handle.net/2115/52360.

(21) Silvius, J.: *Thermotropic phase transitions of pure lipid in model membranes and their*

modifications by membrane proteins; New York: John Wiley & Sons, Inc. 1982.

(22) Ito, D.; Tamate, H.; Nagayama, M.; Uchida, T.; Kudoh, S. N.; Gohara, K. *Neuroscience* **2010**, 171, 50. doi:10.1016/j.neuroscience.2010.08.038.

(23) Mizuno, T.; Kurotani, T.; Komatsu, Y.; Kawanouchi, J.; Kato, H.; Mitsuma, N.; Suzumura, A. *Neuropharmacology* **2004**, 46, 404.

(24) Banno, M.; Mizuno, T.; Kato, H.; Zhang, G.; Kawanokuchi, J.; Wang, J.; Kuno, R.; Jin, S.; Takeuchi, H.; Suzumura, A. *Neuropharmacology* **2005**, 48, 283.

(25) Takeuchi, H.; Mizuno, T.; Zhang, G.; Wang, J.; Kawanokuchi, J.; Kuno, R.; Suzumura, A. *J. Biol. Chem.* **2005**, 280, 10444.

(26) Batenjany, M. M.; Wang, Z.-Q.; Huang, C.-H.; Levin, I. W. *Biochim. Biophys. Acta* **1994**, 1192, 205.

(27) Green, J. L.; Lacey, A. R.; Sceats, M. G. *J. Phys. Chem.* **1986**, 90, 3958.

(28) Maeda, Y.; Kakinoki, K.; Kitano, H. *J. Raman Spectroscopy* **1996**, 27, 425.

(29) Fox, C. B.; Uibel, R. H.; Harris, J. M. *J. Phys. Chem. B* **2007**, 111, 11428.

(30) Ewing, G. J.; Ionescu, L. G. *J. Chem. Eng. Data* **1974**, 19, 367.

(31) Hamada, K.; Fujita, K.; Smith, N. I.; Kobayashi, M.; Inouye, Y.; Kawata, S. *J. Biomed. Opt.* **2008**, 13, 044027.

(32) Jango, M.; Davydovskaya, P.; Bauer, M.; Zink, A.; Stark, R. W. *Opt. Lett.* **2010**, 35, 2765.

(33) Tanaka, S.; Iimura, H.; Sugiyama, T. *J. Soc. Cosmet. Chem. Japan* **1992**, 25, 232 (in Japanese with English abstract).

(34) Wang, H.; Ma, F.; Wang, F.; Liu, D.; Li, X.; Du, S. *J. TRAUMA* **2011**, 71, 1246.

(35) Ajito, K.; Torimitsu, K. *Lab Chip* **2002**, 2, 11.

(36) Uchida, T.; Ebinuma, T.; Takeya, S.; Nagao, J.; Narita, H. *J. Phys. Chem. B* **2002**, 106, 820. doi:10.1021/jp012823w.

(37) Uchida, T.; Ebinuma, T.; Ishizaki, T. *J. Phys. Chem. B* **1999**, 103, 3659. doi: 10.1021/jp984559l.

(38) Uchida, T.; Takeya, S.; Chuvilin, E. M.; Ohmura, R.; Nagao, J.; Yakushev, V. S.; Istomin, V. A.; Minagawa, H.; Ebinuma, T.; Narita, H. *J. Geophys. Res.* **2004**, 109, B05206. doi:10.1029/2003JB002771.

16

Figure captions

Fig. 1: A typical feature of DEPC liposomes (large multilamellar vesicle): (a) optical microscopic image (scale bar 20 μm), and (b) FEG-TEM image of the freeze-fractured replica of the vesicle (scale bar 500 nm). A part of this vesicle has been removed with the freeze-fracture process[17], and its cross section (thick arrow) shows the multiple DEPC layers. The typical stripped pattern and the island structures are observed on parts of the surface.

Fig. 2: Phase contrast image of 34 DIV cultured neurons used for the Raman spectroscopic measurement (scale bar 100 μm).

Fig. 3: Typical temperature (solid line) and pressure (dashed line) conditions during Raman spectroscopic measurements on DEPC liposomes.

Fig. 4: Typical Raman spectra of DEPC liposome solutions at wave numbers (a) lower than 2000 cm^{-1} and (b) higher than 2000 cm^{-1} during temperature decrease process under atmospheric pressure or 0.50 MPa Xe pressure. Solid lines are Raman spectra under 0.5 MPa Xe pressure (thin black line: 282.4 K; thick black line: 280.6 K; thin gray line: 278.8 K), and dotted and dashed lines are under atmospheric pressure (gray dotted line: 292.8 K; black dashed line: 282.3 K).

Fig. 5: Extended Raman spectra of DEPC liposomes on the methylene C-H stretching mode at various temperature and pressure conditions. The legend is the same as in Fig. 4.

Fig. 6: Temperature dependence of Raman peak wave numbers of DEPC liposomes on the methylene C-H stretching mode: (a) C-H symmetric stretching mode (lowest wave number around 2850 cm^{-1}) at atmospheric pressure (open circles) and at 0.5 MPa Xe pressure (solid circles), (b) C-H anti-symmetric stretching mode (middle wavenumber around 2880 cm^{-1}) at atmospheric pressure

18

(open squares) and at 0.5 MPa Xe pressure (solid squares). Each dashed line shows the estimated phase transition temperature.

Fig. 7: Pressure dependence of phase transition temperature (T_m) of DEPC liposomes obtained in the present study (solid circles) and in a previous study (open diamonds)[18] under Xe pressure. Solid triangle shows the phase transition temperature under N_2 pressure. Open circle shows the phase transition temperature under Xe-N_2 mixed-gas condition. This point shifts to lower pressure conditions when the partial Xe pressure is considered (shown by the dotted arrow). The dashed line shows the regression line of T_m with respect to the partial Xe pressure. Error bar shows the uncertainty in the temperature in the step-wise process.

Fig. 8: Extended Raman spectra of DEPC liposomes for the O-D stretching mode at various temperature and pressure conditions. The legend is the same as in Fig. 4b.

Fig. 9: Typical Raman spectra of cultured neuronal network at wave numbers (a) lower than 2000 cm^{-1} and (b) higher than 2000 cm^{-1} during temperature decrease process under atmospheric pressure or 0.57 MPa Xe pressure. The large peaks at around 400 cm^{-1} and 900 cm^{-1} are background peaks from the glass plate. (Dotted gray line: 293.7K at atmospheric pressure; solid gray line: 293.7K at 0.6 MPa; solid black line: 287.1K at 0.57 MPa; solid thick black line: 283.2K at 0.57 MPa; dashed black line: 281.2K at 0.57 MPa; dashed gray line: 277.5K at 0.57MPa.)

Fig. 10: Extended Raman spectra of cultured neuronal network for the methylene C-H stretching mode at various temperature and pressure conditions. The legend is the same as in Fig. 9.

Fig. 11: Pressure dependence of phase transition temperature (T_m) of cultured neuronal network obtained in the present study (solid circles). Dashed line shows the regression line for T_m for DEPC liposomes under the partial Xe pressure (obtained in Fig. 7). Solid line shows the equilibrium condition of Xe hydrates.[30]

Fig. 12: Extended Raman spectra of cultured neuronal network for the O-H stretching mode at various temperature and pressure conditions. The legend is the same as in Fig. 9.

Fig. 13: Pressure dependence of the temperature (T_w) denoted by anomalous change in the Raman intensity ratio in the O-H stretching mode (I_{3270}/I_{3400}). Dashed line shows the regression line of T_m for DEPC liposomes under the partial Xe pressure (obtained in Fig. 7). Solid line shows the equilibrium condition of Xe hydrate. [30]
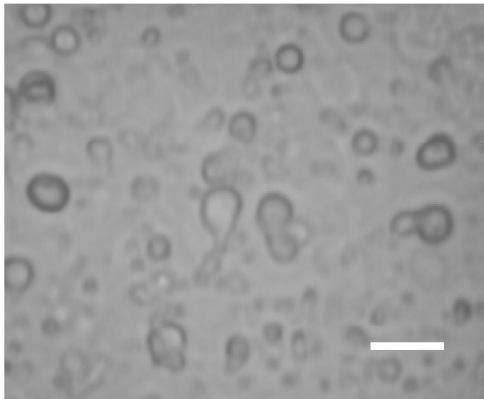
(a) (b)
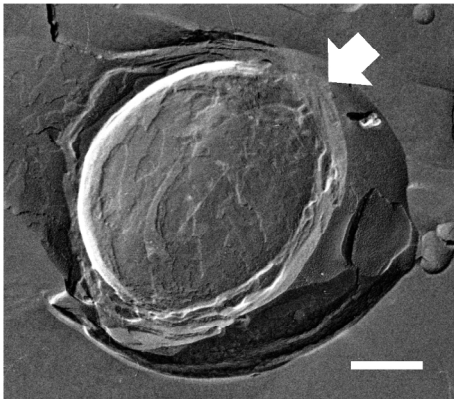
212x97mm (300 x 300 DPI)
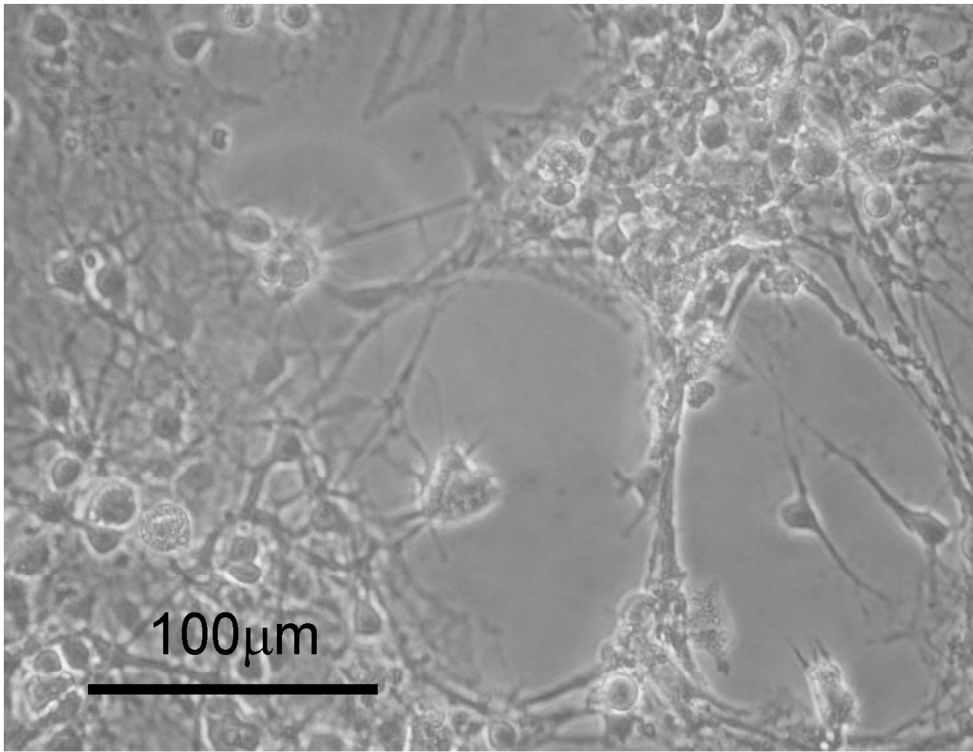
131x102mm (300 x 300 DPI)
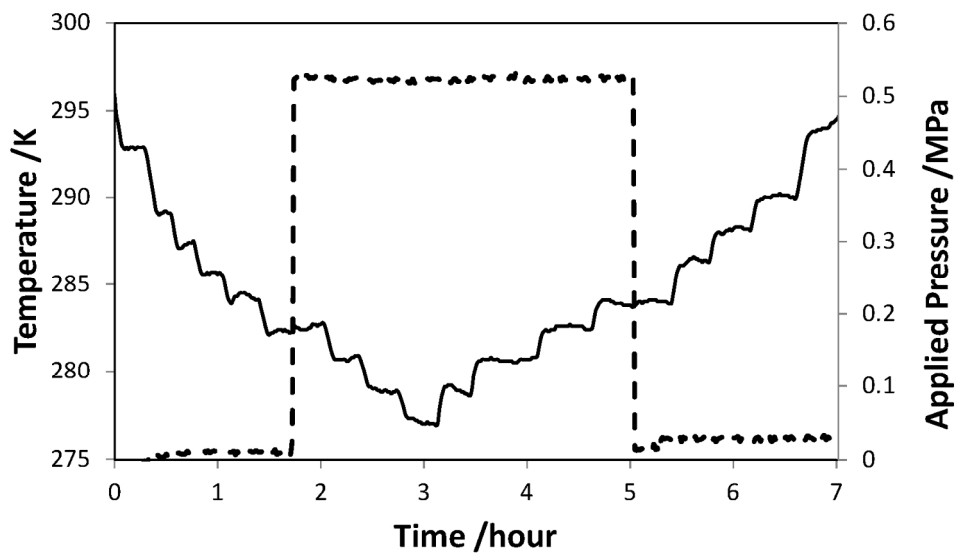
162x94mm (300 x 300 DPI)
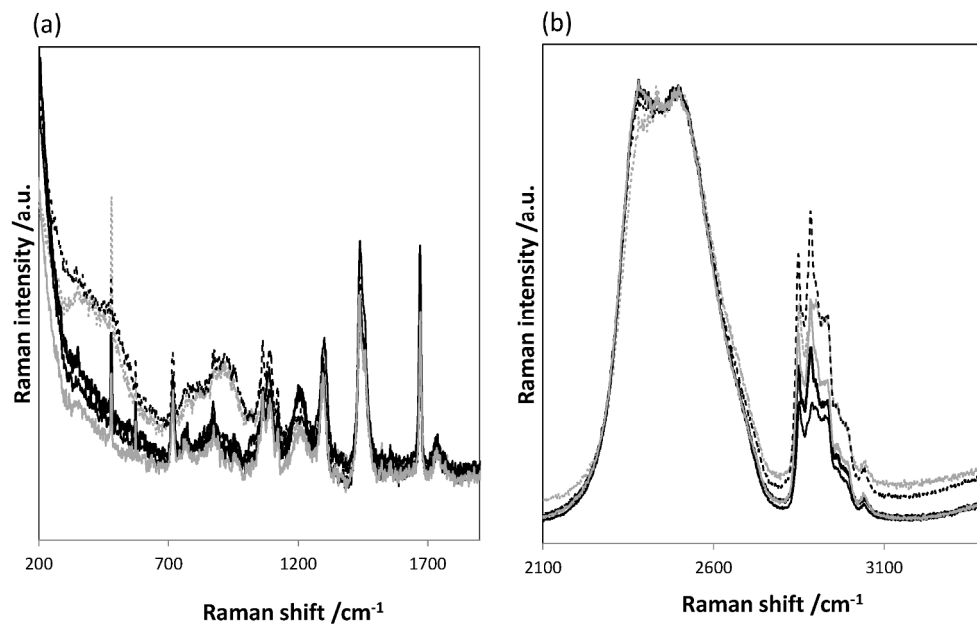
228x141mm (300 x 300 DPI)
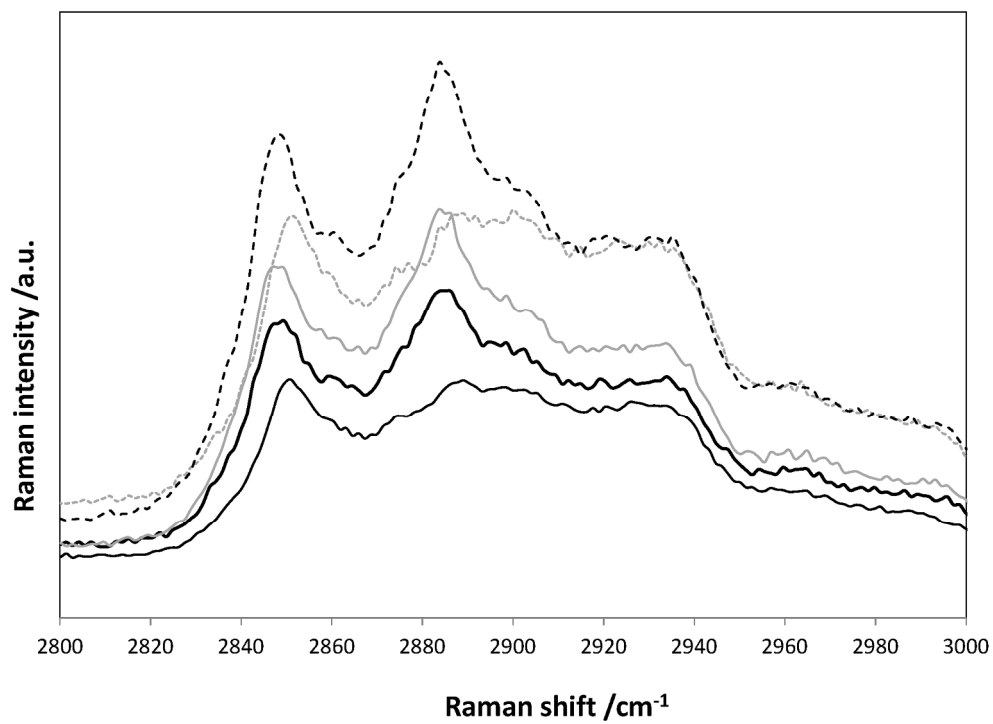
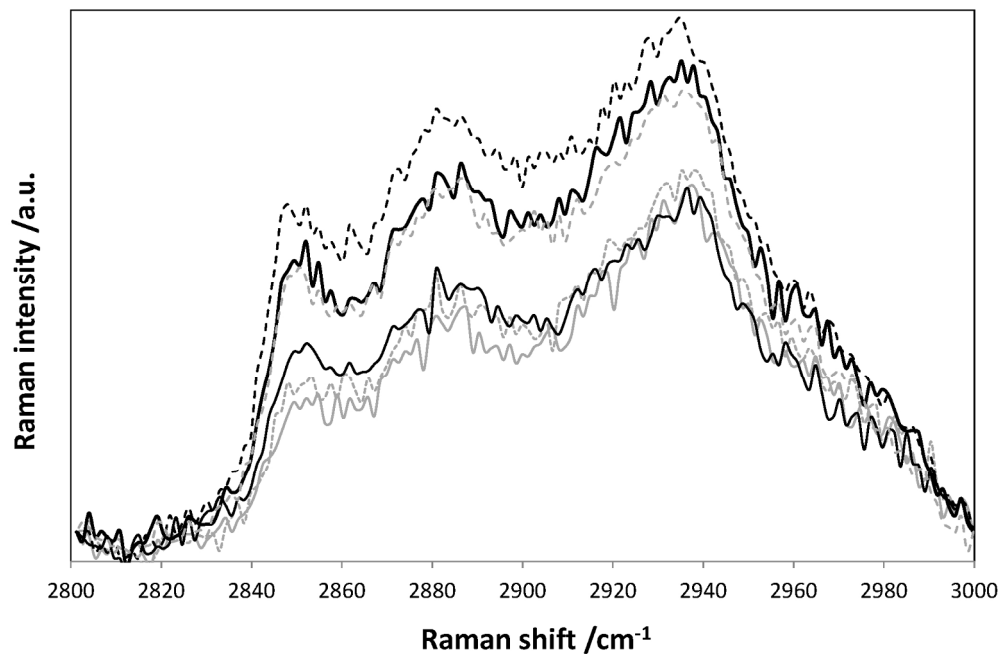184x136mm (300 x 300 DPI)
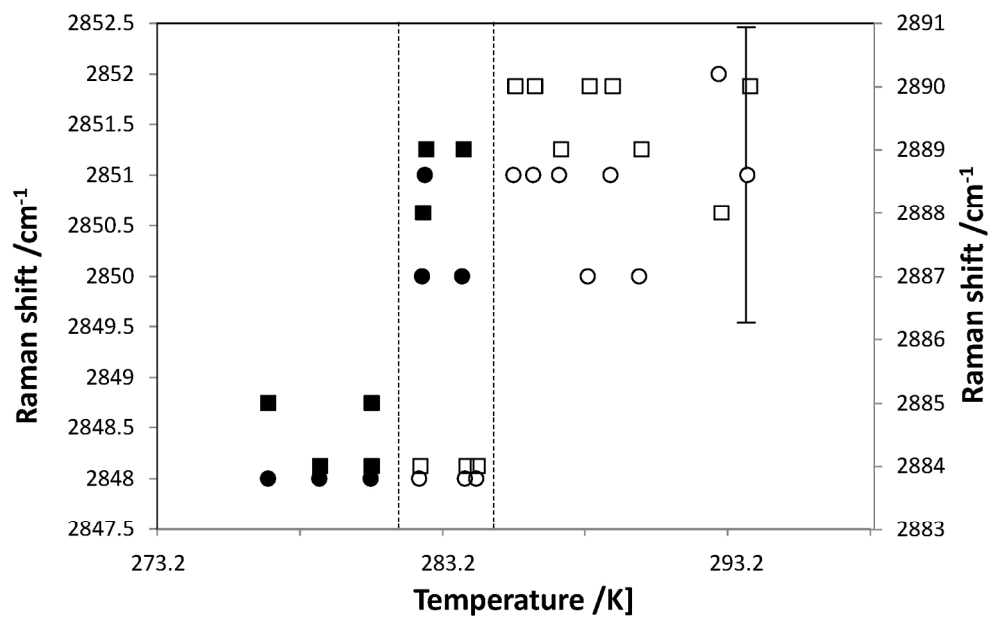
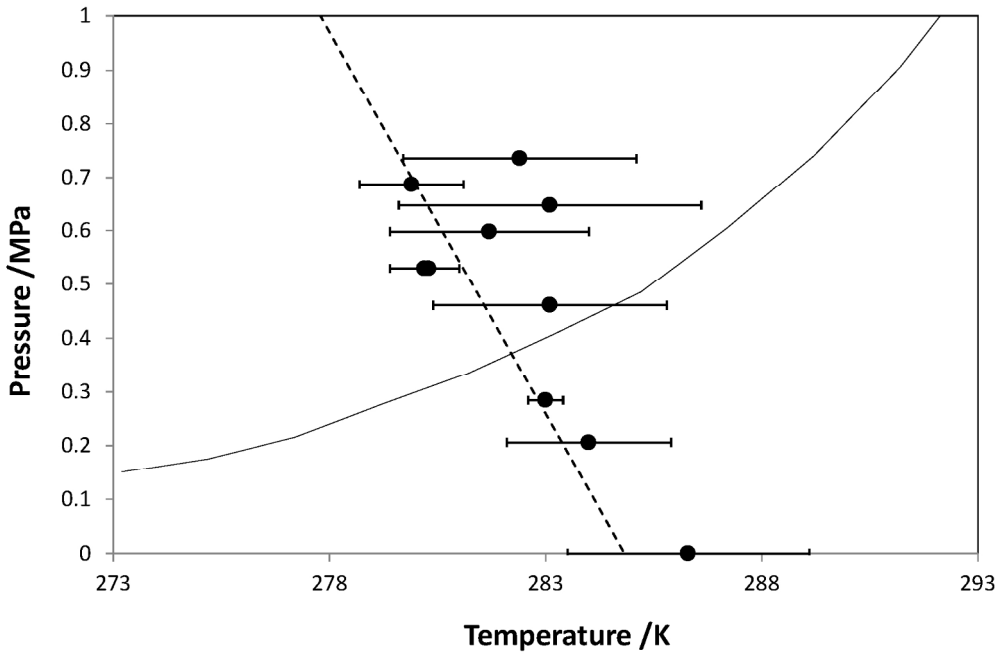174x109mm (300 x 300 DPI)
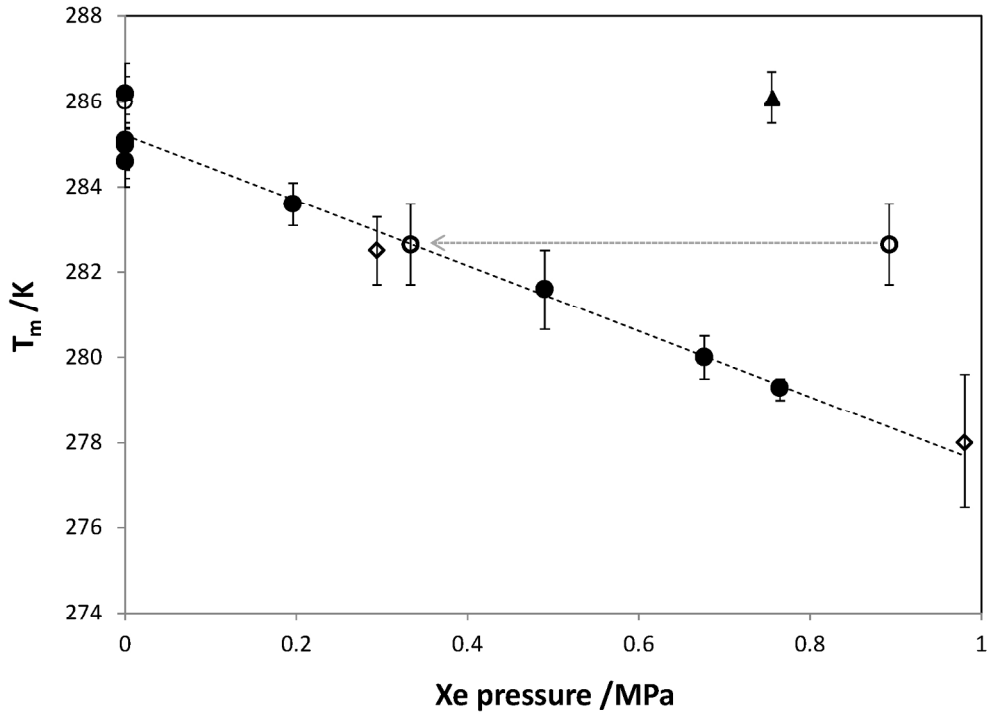
173x125mm (300 x 300 DPI)
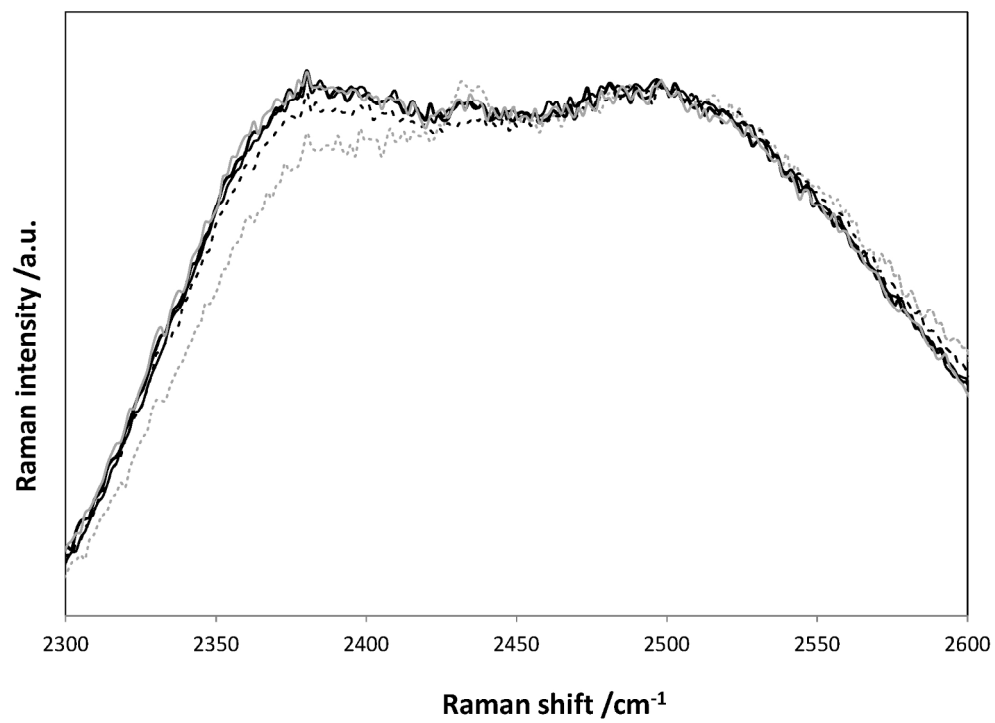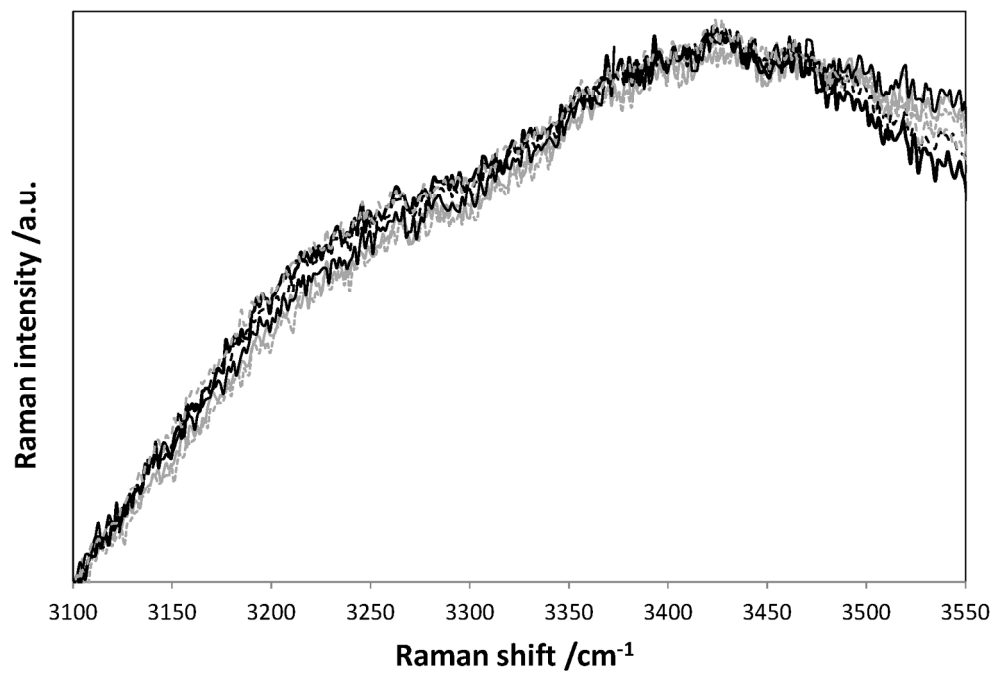
184x134mm (300 x 300 DPI)

(a)

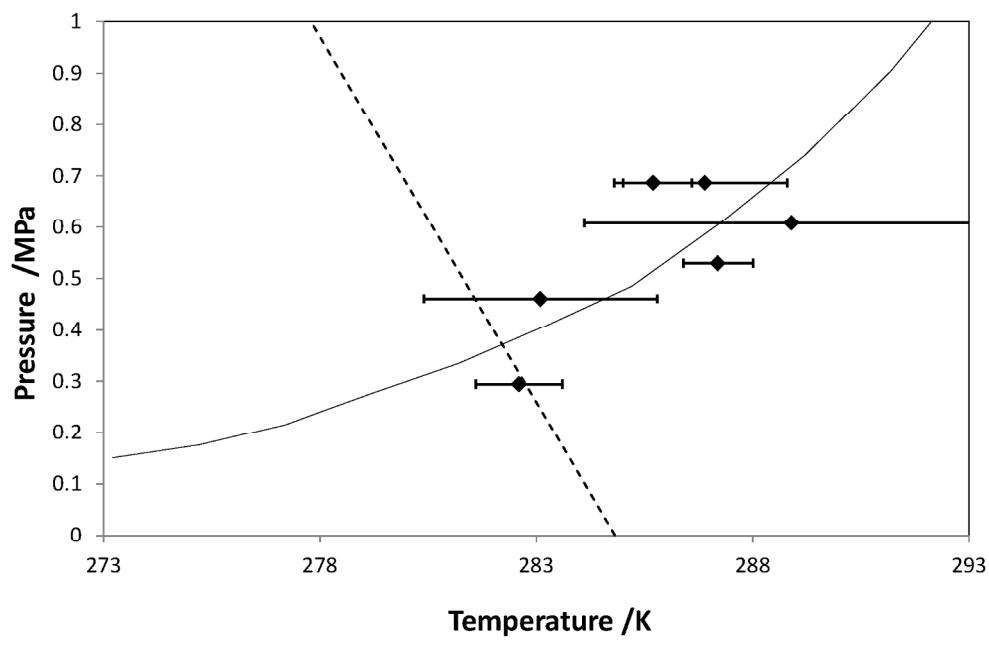(b)
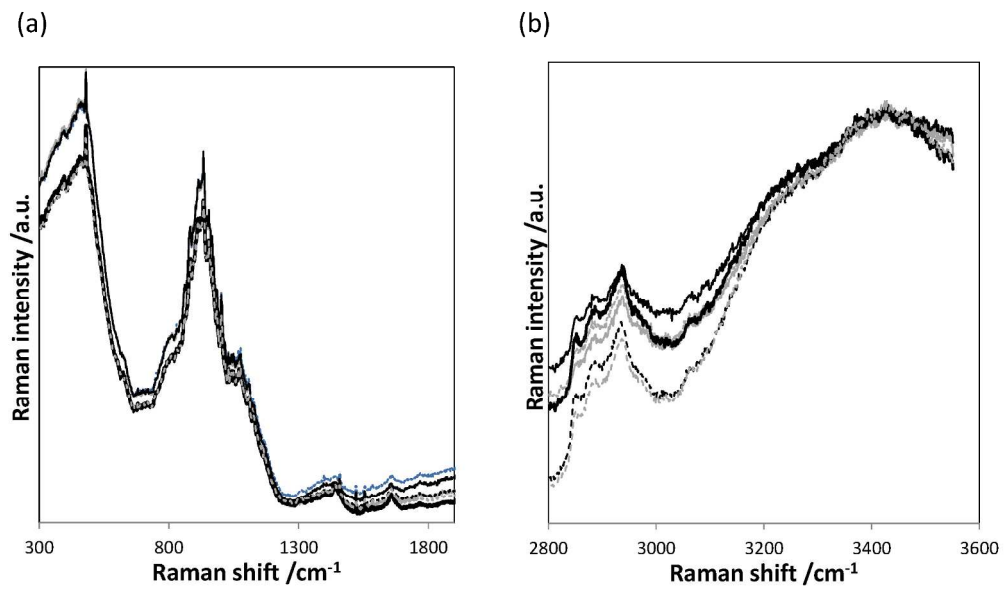
219x130mm (300 x 300 DPI)

180x119mm (300 x 300 DPI)

178x117mm (300 x 300 DPI)

173x119mm (300 x 300 DPI)

181x115mm (300 x 300 DPI)